Düzce Üniversitesi Bilim ve Teknoloji Dergisi

An Assessment of Chromium (VI) Removal from Aqueous Solution Using Gelatin/PAAm-based IPN Hydrogels

Gülen Oytun AKALIN [a,*]

[a] *Tıbbi Hizmetler ve Teknikler Bölümü, Sağlık Hizmetleri Meslek Yüksekokulu, Aksaray Üniversitesi, 68100 Aksaray, Turkey*
* *Sorumlu yazarın e-posta adresi: gulenoytunakalin@hotmail.com*
DOI: 10.29130/dubited.949714

ABSTRACT

In this work, gelatin (G)-polyacrylamide (PAAm)-based interpenetrating polymer network (IPN) hydrogels involving maleic acid (MA) was prepared using by free radical polymerization. Full-IPN and semi-IPN hydrogels were synthesized by using glutaraldehyde and ethylene glycol dimethacrylate (EGDMA) as a crosslinker. The water absorbency of hydrogels was investigated, and the values increased with MA and G. The chemical structures of IPN hydrogels were tested by Fourier Transform Infrared Spectroscopy (FTIR). Morphological test was done by using Scanning Electron Microscope/ Energy Dispersive X-ray Spectroscopy (SEM/EDX). Thermal properties were examined with Differential scanning calorimeter (DSC) analyzer and Thermogravimetric analysis (TGA). The mechanical analysis was performed with Universal Testing Machine. The degradation behavior of hydrogels was investigated against pH. According to the results, IPN hydrogels had good water absorbency capability, degradation, mechanical, and thermal stabilities. The values of full-IPN hydrogel were higher than semi-IPN. The efficiency of adsorption parameters (contact time, initial feed concentration, and pH) on Chromium (VI) ion adsorbing property of IPN hydrogels were also determined. The adsorption increased with increasing initial Cr (VI) concentration from 30 to 150 mg/L. The adsorption was influenced with pH and the maximum adsorption was obtained at pH 6 at 25°C and 80 mg/L Cr (VI) concentration. The effect of contact time on the adsorption was also performed at same conditions. A remarkable increase in Cr (VI) adsorption occurred up to 300 min and then reached at constant value. The adsorption data obeyed Langmuir and Freundlich sorption isotherms. Langmuir isotherm was a better mathematical fit for equilibrium data than Freundlich isotherm, depended on its higher correlation coefficient. Langmuir adsorption capacity (Q) was determined to be 555.55 and 322.58 mg/g for semi-IPN and full-IPN, respectively. Freundlich constants (K_f), an adsorption capacity, were found to be 15.44 and 18.47 for semi-IPN and full-IPN, respectively. According to these results, it can be said that the hydrogel surface was homogeneous, and the adsorption of Cr (VI) occurred in a monolayer.

Keywords: *Polyacrylamide, Gelatin, Hydrogel, Adsorption, chromium (VI), Metal removal*

Jelatin/PAAm-tabanlı IPN Hidrojelleri Kullanarak Sulu Çözeltiden Krom (VI) Uzaklaştırmasının Değerlendirmesi

ÖZET

Bu çalışmada, jelatin (G) -poliakrilamid (PAAm) bazlı, maleik asit (MA) içeren iç içe geçen polimer ağı (IPN) hidrojelleri, radikal polimerizasyon kullanılarak hazırlanmıştır. Tam-IPN ve yarı-IPN hidrojeller, çapraz bağlayıcı olarak glutaraldehit ve etilen glikol dimetakrilat (EGDMA) kullanılarak sentezlendi. Hidrojellerin su emiciliği incelendi ve değerler MA ve G ile arttı. Tam IPN ve yarı IPN hidrojellerin kimyasal yapıları Fourier Dönüşümü

Kızılötesi Spektroskopisi (FTIR) ile test edildi. Taramalı Elektron Mikroskobu/ Enerji Dağılımlı X-ışını Spektroskopisi (SEM/EDX) kullanılarak morfolojik test yapıldı. Termal özellikler Diferansiyel taramalı kalorimetre (DSC) analizörü ve Termogravimetrik analiz (TGA) ile incelenmiştir. Mekanik analiz, Universal Test Makinesi ile yapıldı. Hidrojellerin bozunma davranışı pH'a karşı incelenmiştir. Sonuçlara göre, IPN hidrojellerinin iyi su emme kapasitesi, bozunma, mekanik ve termal kararlılığa sahipti. Tam IPN hidrojelin değerleri yarı IPN'den daha yüksekti. Adsorpsiyon parametrelerinin (temas süresi, başlangıç besleme konsantrasyonu ve pH) IPN hidrojellerinin Krom (VI) iyonu adsorplama özelliği üzerindeki etkinliği de belirlendi. Adsorpsiyon, başlangıç Cr (VI) konsantrasyonunun 30'dan 150 mg/L'ye artmasıyla arttı. Adsorpsiyon pH'dan etkilenmiş ve maksimum adsorpsiyon pH 6'da 25oC'de ve 80 mg/L Cr (VI) konsantrasyonunda elde edilmiştir. Temas süresinin adsorpsiyon üzerindeki etkisi de aynı koşullarda gerçekleştirilmiştir. 300 dakikaya kadar Cr (VI) adsorpsiyonunda kayda değer bir artış meydana geldi ve daha sonra sabit değere ulaştı. Adsorpsiyon verileri Langmuir ve Freundlich sorpsiyon izotermlerine uymuştur. Langmuir izotermi, daha yüksek korelasyon katsayısına bağlı olarak, denge verileri için Freundlich izoterminden daha iyi bir matematiksel uyumdu. Langmuir adsorpsiyon kapasitesi (Q), yarı-IPN ve tam-IPN için sırasıyla 555.55 ve 322.58 mg/g olarak belirlendi. Bir adsorpsiyon kapasitesi olan Freundlich sabitleri (Kf), yarı-IPN ve tam-IPN için sırasıyla 15.44 ve 18.47 olarak bulundu. Sonuçlara göre, hidrojel yüzeyinin homojen olduğu ve Cr (VI) adsorpsiyonunun bir tek tabakada meydana geldiği söylenebilir.

Anahtar Kelimeler: Poliakrilamid, Jelatin, Hidrojel, Adsorpsiyon, krom (VI), Metal uzaklaştırma

I. INTRODUCTION

Hydrogels involving polymer backbone (s), crosslinker(s), and water are high molecular weight three-dimensional network structures Their most characteristic feature is that they can swell in water and shrink in the lack of water. Swelling depends on the crosslink density and hydrophilicity of the structure [1]. Generally, ionizable functional groups (such as carboxylic acid) increase the hydrophilicity and so, the swelling capacity enhances. The increment of counter ions produces an additional osmotic pressure. Due to these structural properties, hydrogels can absorb large amounts of aqueous solutions. They can be utilized in several fields including drug delivery systems, enzyme systems, medical supplies [2].

Full-Interpenetrating polymer networks (full-IPN) hydrogels are consisting of two crosslinked polymers, while semi-Interpenetrating polymer networks (semi-IPN) hydrogels are contained one crosslinked polymer. The thermal and mechanical stabilities of polymeric material can be advanced by preparing IPNs. IPNs have certain inimitable features like easy production into different geometric forms. For this reason, they are used in some biomedical practice; stability against biological fluids, minimal irritation to surrounding tissues, soft and rubbery tissue production, etc. They are also used for controlled release kinetic and the control of hydrophilicity [3]- [5].

Adsorption study is used for the removal of heavy metal ions, due to the economic aspects, ease of operation, convenience, and removal effectiveness. In recent years, the crosslinked polymeric materials, which have functional groups such as carboxylic acid, hydroxyl amine, and sulfonic acid groups, have been used as a support material for the removal of metal ions from aqueous solutions. These functional groups within the polymeric matrix bind with the metal ions to provide the formation of complex structures and so, heavy metal ions easy remove from the environment. For this purpose, ionic polyacrylamide (PAAm) gels have been widely used in recent years [6]. Additionally, it is used as the main ingredient in hydrogels designed for drug release, due to its high biocompatibility and easy manufacturing property. It has good permeability to hydrophobic and hydrophilic substances [2], [7]. Depending on the crosslinking density, it can increase the mechanical strength of structure. Biopolymers such as gelatin (G) are commonly used for adsorption studies to obtain low-cost and non-toxic adsorbent materials. It has biodegradable nature, easy availability, bioadhesive, and gelation properties. According to literature, its functional groups (hydroxyl, amino, and carboxyl) act as an active site for the target ionic species [8], [9]. These groups play a fundamental role in bonding with ionic species such as metal ions. The ionic or polar interaction between functional groups and metal ions ensures the removal of metal ions from the environment [9]. Thus, G has a good bioadsorbent properties. G has been used in many studies to remove Chromium (VI) ions as a bioadsorbent [10]-12]. It is widely worked because of

its biodegradability, low cost, non-immunogenic, and biocompatibility qualities [2]. It is extremely utilized in biomedical industry such as adsorbent pad, wound dressing, microspheres, hard and soft capsules etc. It is easily chemically crosslinked with crosslinker due to having the several number of functional groups [7], [13], [14]. Maleic acid (MA) is a dicarboxylic acid, and it is utilized as a pH adjuster and fragrance ingredient, especially in cosmetics. MA is disclosed as legal indirect ingredient in the food industry [15]. It is commonly used the removal of heavy metal ions. According to the literature, the carboxyl groups of maleic acid can be easily bonded with heavy metal ions by electrostatic interaction [16]. Thus, heavy metal ions easily remove from the environment [17].

Effective uptake of heavy metal ions from water is a vital environmental research topic. Chromium (VI) is one of the high toxic metal ions even at extremely low concentrations. It enters the environment from the industries process like leather tanning, electroplating, paint, cement, dyes, ink, and textiles. Furthermore, it causes health risks such as dermatitis, gastrointestinal ulcers, and liver damage. Many methods such as reverse osmosis, chemical reduction, precipitation, electro dialysis and ion exchange are used to remove chromium (VI) [18]. These methods have some disadvantages, for example, such as the formation of large contents of toxic waste sludge, incomplete metal removal, and high energy requirements.

In this study, it was aimed to synthesize effectual hydrogel that could exactly the remove of Cr (VI) metal ion from water. PAAm and PAAm/G, full-IPN (PAAm/G/MA-1) hydrogel, and semi-IPN (PAAm/G/MA-2) hydrogel were prepared. The characterization of hydrogels was performed by FTIR, SEM/EDX, TGA, DSC and Universal Testing Machine. The water absorbency and degradation behavior of hydrogels were also researched. Full-IPN and semi-IPN hydrogel were utilized as an adsorbent for the removal of Cr (VI) from aqueous solution by the assessment of initial feed concentration, contact time and pH parameters.

,

II. MATERIALS AND METHODS

A. MATERIALS

Gelatin (G; Type B, 280 Bloom, from pig skin), acrylamide (Aam; for molecular biology, purity≥99%), maleic acid (MA; ~99%, analytical reagent grade), glutaraldehyde (25% aqueous solution, GA), ethylene glycol dimethacrylate (EGDMA; ~98%), ammonium persulfate ($(NH_4)_2S_2O_8$, ACS reagent, ≥98.0%), and sodium metabisulfite ($Na_2S_2O_5$, reagent grade, 97%) were obtained from Sigma-Aldrich. Double deionized water was utilized in the synthesis procedure of IPN hydrogels and metal adsorption test [19].

B. METHODS

B. 1. Full-IPN and Semi-IPN Hydrogels Preparation

Full-IPN and Semi-IPN hydrogels were synthesized by radical polymerization. The reaction was started by using $(NH_4)_2S_2O_8/Na_2S_2O_5$ redox pair at 25°C for both hydrogel synthesis. While the full-IPN hydrogel had two crosslinking agents (GA and EGDMA), semi-IPN hydrogel was involved one cross-linking agent, only EGDMA. GA was used for crosslinking of G and EGDMA was utilized for crosslinking of PAAm.

Synthesize Procedure: Around 4.00 mL of 6.0 M AAm solutions was added into 10% G solutions and MA (0.08 g) with different volumes of crosslinkers. After the adding two initiators (0.02/0.02 g/g), the mixture was taken into tubes. The mixture was left at room conditions for 24 h to complete the reaction. The tubes were broken and then samples were cut to obtain pieces with a length of 0.5 cm. After washing process, the cylindrical type hydrogels were dried at 25°C and then, at 40°C in a vacuum oven. Dried

samples were stored at room temperature. The contents of components are presented in Table 1. The Full-IPN hydrogel preparation method is given schematically in Fig. 1.

Table 1. The contents of components used for hydrogel synthesis procedure.

Hydrogel	AAm (g)	G (ml)	MA (g)	EGDMA (ml)	GA (ml)
PAAm	1.70		-	0.04	-
PAAm/G	1.70	1.28	-	0.04	-
(PAAm/G/MA)-1	1.70	1.28	0.08	0.04	-
(PAAm/G/MA)-2	1.70	1. 28	0.08	0.04	0.3
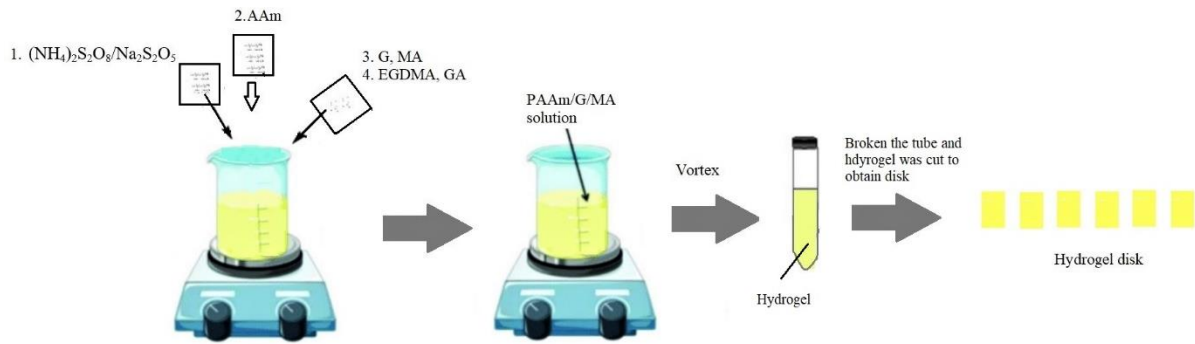
Figure 1. Schematic diagram of formation of Full-IPN hydrogel.

B. 2. Characterization

FTIR, SEM, thermal and mechanical tests were performed at Duzce University Scientific and Technological Application and Research Center.

B. 2. 1. FTIR analysis

FTIR spectrum of AAm, G, MA, (PAAm/G/MA)-1 and (PAAm/G/MA)-2 samples were obtained from FT-IR Shimadzu IR-Prestige 21. Approximately 1 mg of the pounded samples were blended with KBr. The hydraulic press was utilized for generation of pellets. The pressure was arranged at 600 kg/cm^2. Spectrum were scanned between 400 and 4000 cm^{-1} [7], [13].

B. 2. 2. Water absorbency test

Dry hydrogels of known weight (w_d) were placed in distilled water (at 25°C and pH 7.0). The swollen hydrogels that were taken at different times were weighed (w_s) after wiping with filter paper. The weighing was done by the time it reached a constant weight. The experiment was repeated three times. Equation (1) is used to calculate the water absorbency [2], [7]:

$$\text{Water absorbency } (\%) = \frac{(w_s - w_d)}{w_d} x100 \tag{1}$$

B. 2. 3. Degradation test

The in vitro degradation studies of hydrogels were performed in phosphate buffer solution (PBS) at different pH [20]. Samples were placed in vials, each containing 25 mL PBS. At predetermined time, hydrogels were picked out of PBS, the residual water was wiped off from the sample surface and then,

the samples were weighted [21]. The weighing was performed at 25°C and 120 h (according to water absorbency results).

The degradation (%) was determined as follows [21], [22]:

$$\text{Degradation (\%)} = \frac{(m_i - m_f)}{m_f} x 100 \tag{2}$$

where m_f is the final mass and m_i is the initial mass.

B. 2. 4. SEM/EDX analysis

Surface properties of samples were observed with FEI QUANTA FEG 250 Scanning Electron Microscope (SEM). Investigation of the hydrogels coated with Au/Pd was carried out under 10 kV accelerating voltage [2], [5]. The presence of Cr into the Cr(VI)-loaded (PAAm/G/MA)-2 hydrogel was determined using an Octane Pro Ametek energy-dispersive X-ray (EDX).

B. 2. 5. Thermal analysis

The alteration of the physical properties with temperature was performed by thermal analysis. The mass change of hydrogels was detected with thermogravimetric analysis (TGA). The thermal test was performed by DTG 60 H Shimadzu Simultaneous DTA-TG Apparatus analyzer under dynamic nitrogen atmosphere. Measurements were done at from 20 to 700°C at heating speed of 10°C.min^{-1} [23], [24].

The amount of heat required to increase the temperature of a sample and a reference is determined in Differential scanning calorimetry (DSC) as a function of temperature. DSC-60 Shimadzu Differential Scanning Calorimeter was utilized for this analysis. The range of temperature was 20–700°C (10 °C.min^{-1}) under nitrogen gas atmosphere. The mass losses were evaluated as a function of time and temperature [23], [25].

B. 2. 6. Tensile test

The percentage of elongation at break and the tensile strength of the samples were examined using Universal Testing Machine Type Z 0.5. The elongation values (%) at break were calculated by dividing the sample by the initial length and multiplying by 100. Tensile strength (unit MPa) was found by dividing by the maximum load (N) by the sample cross-section (mm^2). Equation (3) and Equation (4) was used to determine the elongation at break (%) and tensile strength [26].

$$Elongation\ at\ break\ (\%) = \frac{Displacement\ at\ break\ x100}{Gauze\ Length} \tag{3}$$

$$Tensile\ strength\ (MPa) = \frac{Load\ (N)}{Thickness\ (mm)x\ Width\ (mm)} \tag{4}$$

B. 3. Adsorption Studies

A series of experiments were conducted to research the influence of pH, contact time, and initial concentration of metal solution on adsorption. The stock 1000 mg/L of Chromium (VI) solution was obtained by dissolving $K_2Cr_2O_7$ in double distilled water. 50 mg of full-IPN and semi-IPN hydrogels were put into 50 mL of Cr (VI) solution (80 mg/L) [27]. The pH was adjusted with 0.1N NaOH and 0.1N HCl [28]. The solution was shaken continuously at 120 rpm in shaker water bath at 25°C. A certain amount of sample was removed from the solution at certain time intervals for determining of Cr (VI) concentration. The experiment was continued until the equilibrium value was observed. The metal contents were detected by a Shimadzu-18A UV-Visible spectrophotometer) at 540 nm. The adsorbed Cr (VI) ions per unit weight of sample at time t, Q (mg/g), was found from the weight balance equation as [18]:

$$Q = \frac{(C_0 - C_t)\, V}{W} \tag{5}$$

where C_t and C_o are the equilibrium and initial Cr (VI) concentration (mg/L), respectively, W (g) is the weight of sample and V (L) is the volume of solution.

III. RESULTS AND DISCUSSION

The mechanism of full-IPN and semi-IPN hydrogels is given in Figure 2. Initially the reduction of the persulfate to the anion radical $(SO_4)^{\cdot-}$ was formed and then, the generation of vinyl radical from the monomer took place. Finally, the radically polymerization were occurred. In semi-IPN structure, G was the guest polymer and PAAm was host polymer. The polymer chains were crosslinked with EGDMA. In full-IPN structure, both polymers (G and PAAm) were crosslinked with their crosslinker.
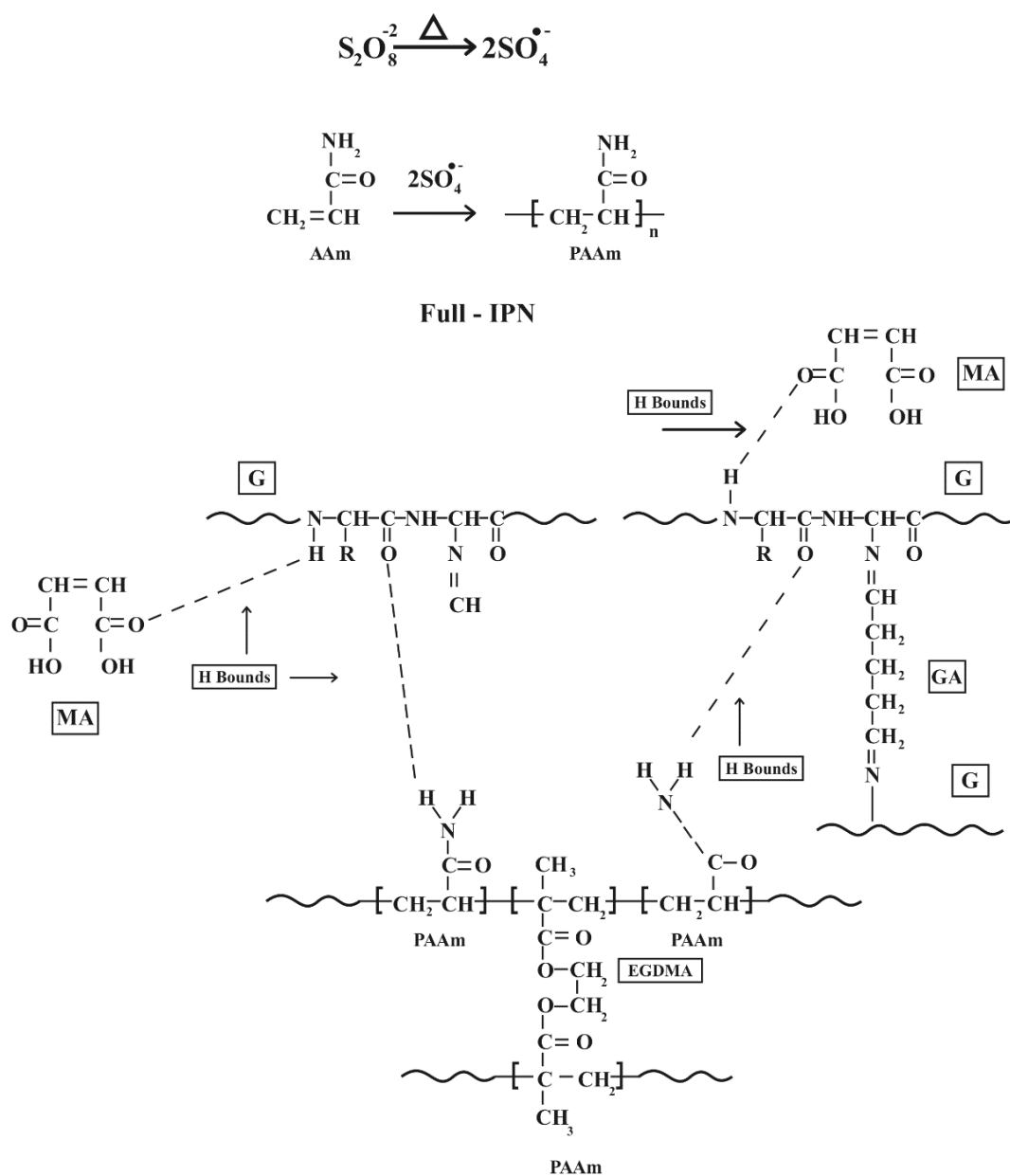
Figure 2. The formation of full-IPN and semi-IPN hydrogels mechanisms.
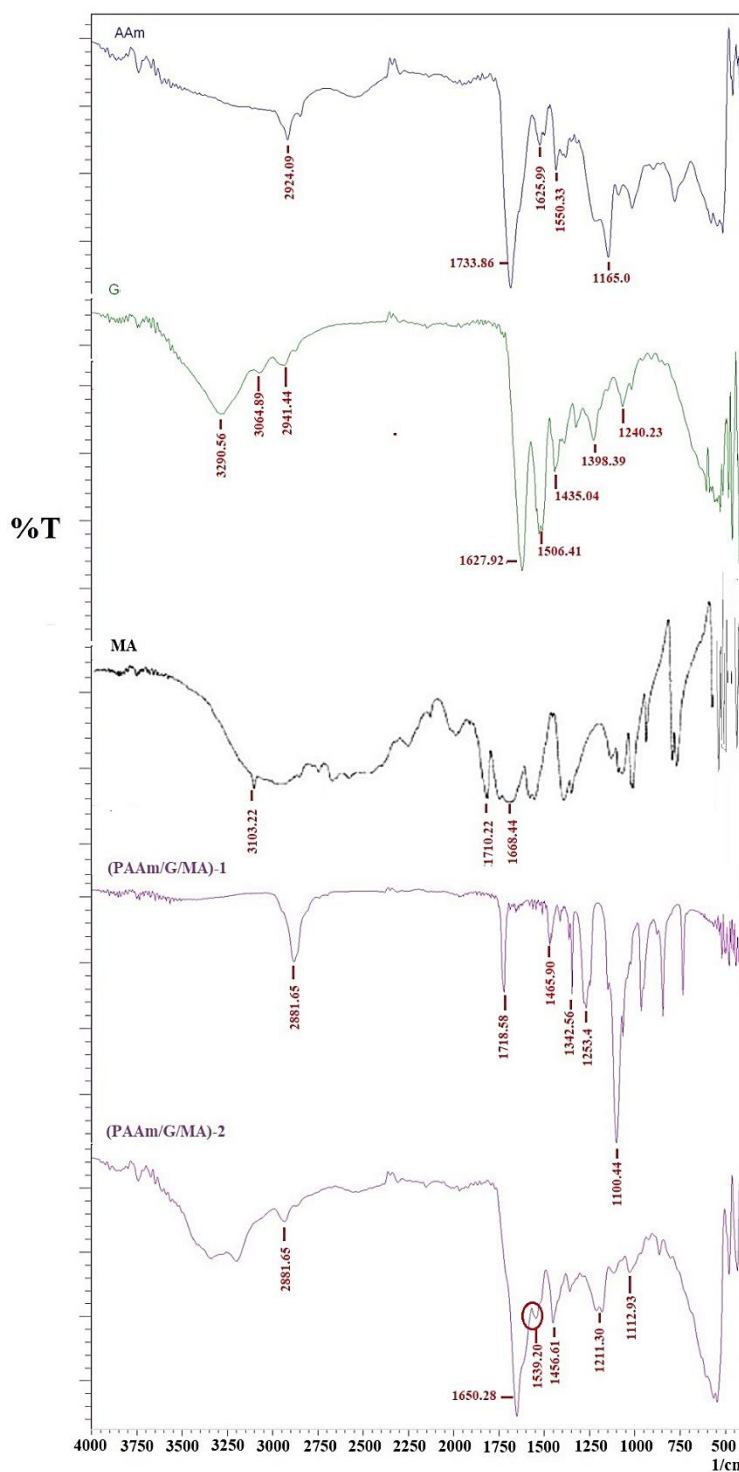
Figure 3. FTIR spectra of AAm, G, MA, full-IPN and semi-IPN hydrogels.

In order to detect the chemical structure of G, AAm, MA, and P(AAm/MA/G) hydrogels, FTIR analysis was performed (Figure 3). MA spectrum displayed the specific absorption broad bands at 3400–2400 cm^{-1} of hydroxyl (-OH) stretch; at 3103.2 cm^{-1} of (vinyl) C-H stretch, at 1668.44 and 1710.22 cm^{-1} of conjugated C=C and C=O [29]. AAm spectrum displayed specific bands at 2924.09, 1625.99 and 1550.33 cm^{-1} because of the existence of C-H aliphatic, C=O and primary amine (N-H bend), respectively [30,31]. In FTIR spectrum of G, the band at 3290.56 cm^{-1} ascribed to the existence of -H

bond of hydroxyl group and -H bond of amide. At 1627.92 cm^{-1} peaks accorded to the existence of amide-I, at 1506.41 cm^{-1} pointed amide-II, band at 1240.23 cm^{-1} pointed out the amide-III, the peaks range from 1435.04 cm^{-1} to 1398.39 cm^{-1} were attributed to the symmetric and asymmetric bending vibrations of -CH$_3$ group [30,31]. (PAAm/G/MA)-1 spectra showed the characteristic bands at 2881.65 and 1718.58 cm^{-1} due to the existence of C-H aliphatic and C=O group, respectively. The absorption band of C-H and O-H bends were observed at 1465.90 and 1342.56 cm^{-1}. The peaks at 1100.44 cm^{-1} were attributed to C–O stretch [7], [32]. The absorption bands at ~3100 cm^{-1} (C-H stretch of vinyl group) and ~1600 cm^{-1} (conjugated C=C) were disappeared. This result can be explained by the formation of semi-IPN hydrogel through CH$_2$=CH– of AAm, -NH$_2$ groups of G, and conjugated C=C of MA. Unlike semi-IPN hydrogel, the peak at ~1540 cm^{-1} was observed in the spectra of full-IPN hydrogel. This result can be explained by the formation of imine bonds (-C=N) because of the crosslinking between the amino group in G and the aldehyde group in GA [31].
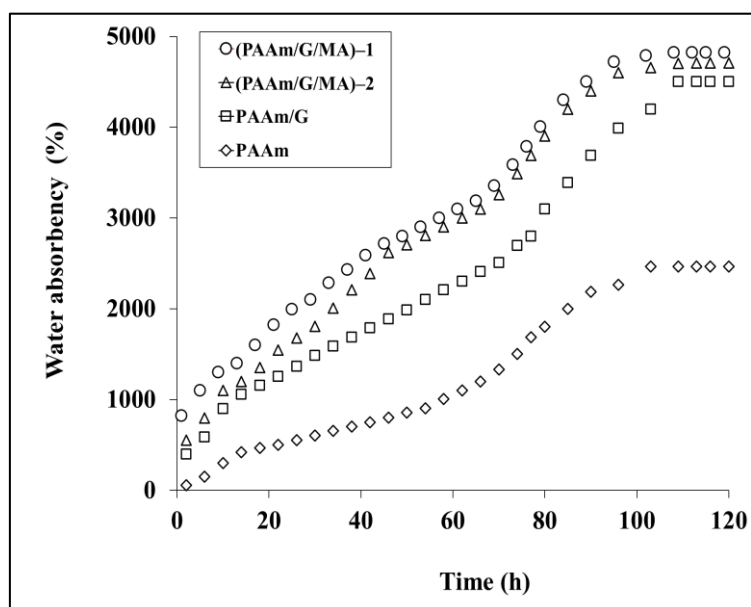
***Figure 4.** The water absorbency (%) of hydrogels with time.*

The water absorbency values were researched, and they were found by plotting as a function of time in Figure 4. When a dried hydrogel is immersed in distilled water, the water penetrates the structure. The diffusion rate depends on chemical and physical properties of the gel sample. In Figure 4, the maximum value was obtained to be nearly 4822% for (PAAm/G/MA)-1 hydrogel, whereas the minimum value was found to be nearly 2466% for PAAm hydrogel. Water absorbency increased rapidly in 10 h, then reached equilibrium value in 120 h. The water absorbency increased with the enhancing of the presence of ionic groups in the structure like diprotic acid. In other words, absorbency increased with the presence of G and MA [5]. This can be explained by the repulsive force that occurs between the electron pair of the N atom and the negatively charged COO$^-$ groups in G and AAm. The full-IPN hydrogel had less water absorption than semi-IPN hydrogel. This can be explained by using two crosslinkers in the full IPN type hydrogel. The presence of two crosslinkers made the structure tighter and this limited the diffusion of water into the structure [33], [34].
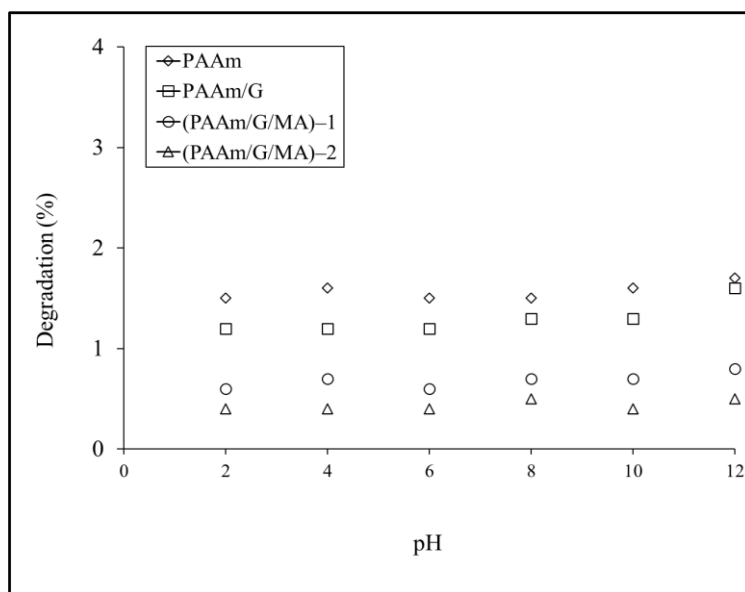
Figure 5. The degradation behavior (%) of hydrogels with pH (at 25°C, 120 h).

The degradation behavior of hydrogels with pH is shown in Figure 5. The degradation (%) were ranged from 0.43% to 1.71%. As pH was increased from 2 to 12, the values were nearly constant. It can be clearly said that all hydrogels had resistant to degradation with pH. Especially, full-IPN hydrogels had high resistance compared to other hydrogels. It can be said that the presence of two crosslinkers in hydrogel structure increases the degradation stability [35,36].

SEM images of dried hydrogel, semi-IPN and full-IPN hydrogels are displayed in Figure 6. The morphological distinctness between dry and swollen samples is obviously appeared. While the surface of swollen samples had pores, dried hydrogel exhibited a nonporous smooth surface. The porosity ensures easy absorption and diffusion of water into structure. The smallest and largest pores were obtained for full-IPN and semi-IPN, respectively. It can be said that the sizes decreased with using two crosslinkers in hydrogel synthesis process. SEM results were in good agreement with water absorbency results. The EDX spectra of the adsorption of Cr (VI) in (PAAm/G/MA)-2 hydrogel is shown in Figure 7. The weight and atomic fraction values are given in Table 2. It has been proven that Cr (VI) adsorbed to the hydrogel.

(a)   **(b)**

(c)

(d)
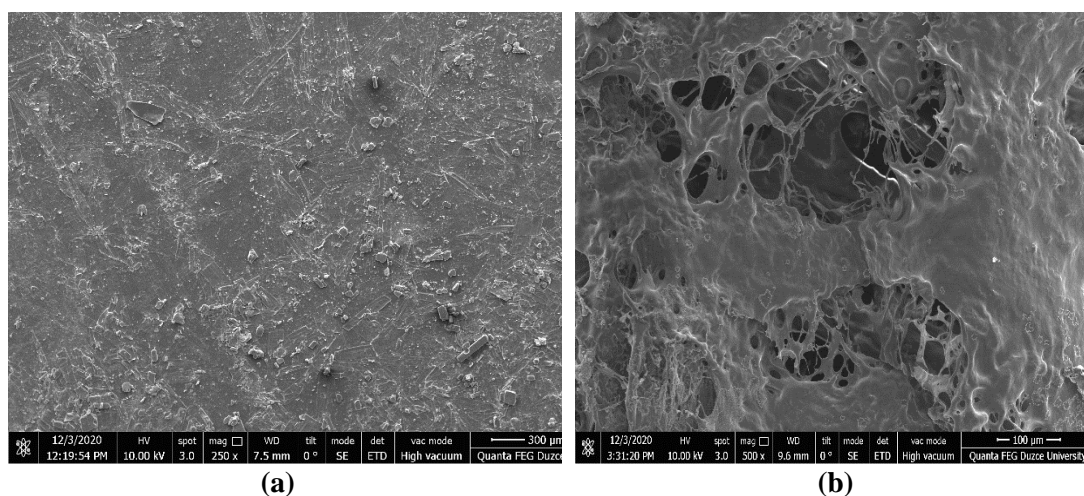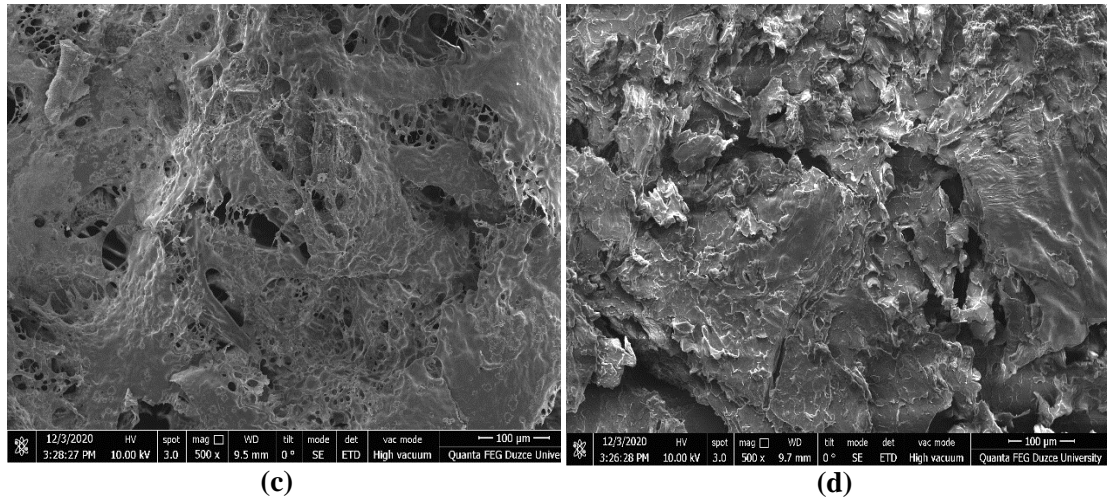
Figure 6. *The surface SEM images of a)* dried hydrogel, *b) swollen (PAAm/G/MA)-1 hydrogel, c) swollen (PAAm/G/MA)-2 hydrogel d) Chromium(VI)-loaded (PAAm/G/MA)-2 hydrogel.*
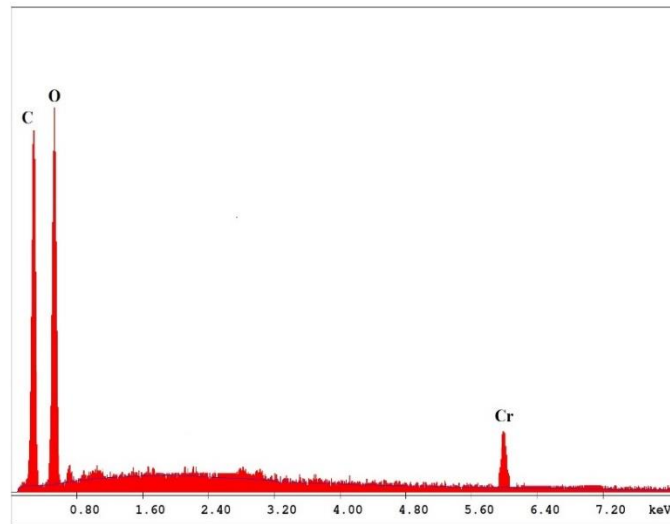
***Figure 7.*** *EDX analysis of Chromium(VI)-loaded (PAAm/G/MA)-2 hydrogel.*

Table 2. *The weight and atomic fraction values of Chromium(VI)-loaded (PAAm/G/MA)-2 hydrogel.*

Element	Wt %	At %
C K	39.7	35.1
O K	50.1	53.5
Cr K	10.2	11.4

The TGA curves of PAAm, PAAm/G, (PAAm/G/MA)-1 and (PAAm/G/MA)-2 hydrogels are shown in Figure 8a. The thermal degradation of the PAAm formed via three stages process. The first stage at 155-220°C was associated with the separation of water absorbed or moisture. The second stage from to 220-298°C was related to the loss of NH_2 of amide side groups in ammonia form by imidization. The third level at 298-455°C was ascribed to the process the main chain dissociation. The degradation of PAAm/G was resembled PAAm. The curves of PAAm/G had three thermal decomposition steps. The first weight loss occurred ranged at 0-155°C because of the elimination of moisture. The second stage was ensued at 165–307°C, the weight loss was associated with thermal decomposition of G and the loss of ammonia by imidization [37]. The third decomposition ranged at 307–460°C was attributed the main chain dissociation. Semi-IPN (PAAm/G/MA)-1 hydrogel had slightly lower thermal stability than

PAAm/G. It exhibited three degradation steps. The first degradation step, was under 230°C, could be related to moisture and the elimination of the carboxylic groups of MA. The second step, from 230 to 326°C was associated with ammonia via dehydration and imidization [38]. The main chain dissociation process occurred in the third stage above 326°C. Full-IPN (PAAm/G/MA)-2 hydrogel degraded in a similar manner. The first weight loss occurred ranged at 0-285°C because of the elimination of the carboxylic groups of MA, and the separation of moisture. The second weight loss, from 285 to 422°C was associated with ammonia via dehydration and imidization. The main chain dissociation process occurred in the third stage above 422°C. Semi-IPN hydrogel completely degraded at 700°C, whereas the full-IPN hydrogel did not completely degraded. It can be said that the generation of full-IPN structure enhanced the thermal stability. The strength of the covalent bond between the atoms formed in the structure may be affected the thermal stability of the polymer material. Therefore, it can be said that the increased thermal stability is evidence of the presence of two crosslinkers in the structure and the formation of covalent bonds.

The DSC curves of PAAm, PAAm/G, (PAAm/G/MA)-1 and (PAAm/G/MA)-2 hydrogels show in Figure 8b. The DSC thermograms were detected to be accordance with the TGA results. Three endothermic peaks were obtained for PAAm. The first endothermic peak was observed at 170°C due to moisture. The second endothermic broad peak may have arisen from the loss of ammonia via imidization in the structure at 230-285°C. According to the literature, the melting temperature (T_m) of PAAm is 273°C and the generation of imide groups occur in this temperature. The third endothermic peak occurring at 320-360°C can be correlated with the glassy temperature (T_g) of the new imide groups of PAAm. In literature, T_g of new imide groups was occurred at 324°C after imidization of PAAm [36]. Three endothermic peaks were obtained for PAAm/G. The first endothermic peak at 100-120°C may have been occurred due to T_g of G and the moisture content in structure. The result was in accordance with the literature. G has low T_g at 116°C and multi high T_g at 145-230°C [39]. The second endothermic broad peak at 220-280°C may have occurred because of the multi T_g of G and imidization. It may have been formed because of phase distinction between G and PAAm or due to the bond disconnection of amino acids with glycine, hydroxyproline and proline in G matrix and generation of imide groups. With respect to literature, the low T_g of G was attributed to the devitrification of the soft blocks α-amino acids with glycine, hydroxyproline and proline while the multi high T_g of G transition was assigned to the devitrification of the rigid amino acids with glycine, hydroxyproline and proline. The third endothermic peak at 330-365°C may be T_g of new imide groups in PAAm matrix [40]. Three endothermic peaks were obtained for semi-IPN hydrogel. The initial broad endotherm temperature at 110 to 125°C could be due to low T_g of G, and moisture content [29]. The second endothermic broad peak at 225-285°C may have occurred because of the multi T_g of G and imidization. The third endothermic peak at 325-345°C may be T_g of new imide groups. Full-IPN hydrogel had three endothermic peaks like semi-IPN hydrogel. The degradation with temperature was slower than semi-IPN, so shift of peaks was observed in the thermogram. Semi-IPN hydrogel was completely degraded at 700°C, whereas the mass loss of full-IPN was observed nearly %90 at 700°C. Therefore, it can be said that full-IPN hydrogel was more resistant to temperature than semi-IPN hydrogel.

(a)   **(b)**
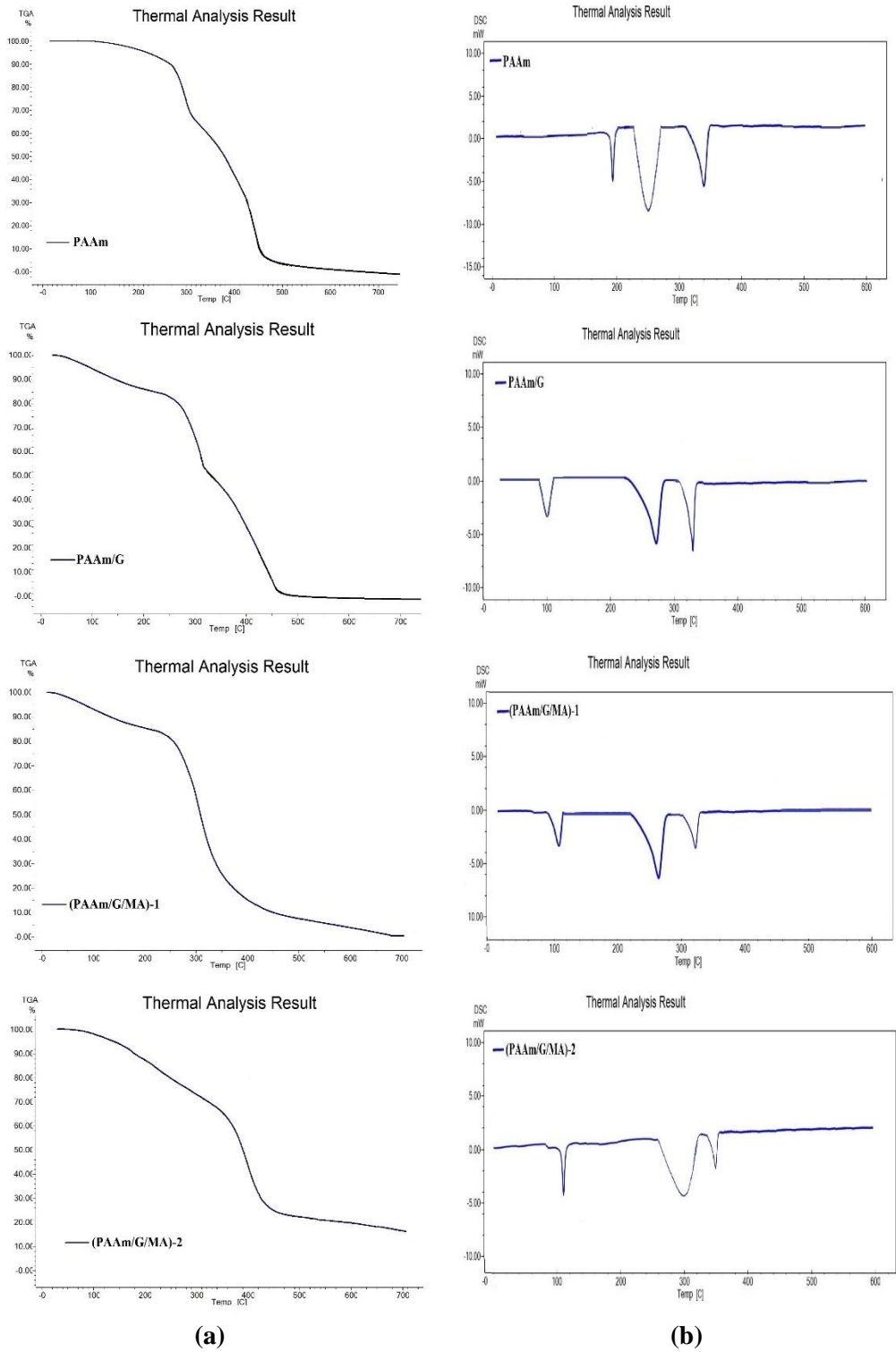
Figure 8. *a) TGA and b) DSC curves of PAAm, PAAm/G, (PAAm/G/MA)-1 and (PAAm/G/MA)-2 hydrogels.*

The mechanical properties of PAAm, PAAm/G, (PAAm/G/MA)-1 and (PAAm/G/MA)-2 hydrogels were examined. Figure 9 displays the elongation (%) at break of hydrogels and tensile strength (M.Pa). No major differences were observed. With preparing full-IPN hydrogel, the tensile strength enhanced from 39.22 MPa to 43.44 MPa and the elongation (%) aroused from 6.77% to 8.35%. It can be said that the addition of crosslinker developed the mechanical stability. This can be explained by the possible molecular interaction that forms when two crosslinking reactions occurs in structure. The intense molecular interactions may be strengthening the structural integrity by enhancing tensile strength [24].
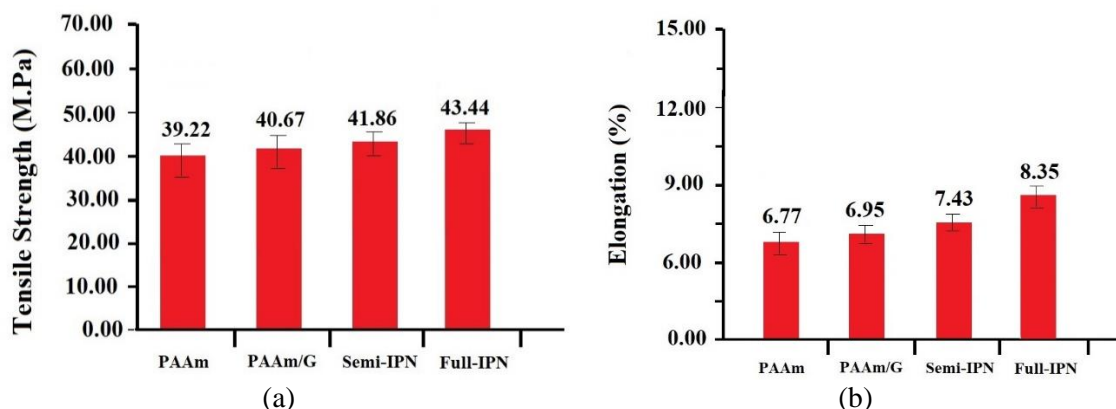
Figure 9. *The mechanical properties of hydrogels (a) tensile strength (M.Pa) and (b) elongation (%). Results shown are mean ± standard deviation, n = 3.*

According to characterization results, the highest thermal and mechanical stability, and good water absorbency were observed for (PAAm/G/MA)-1 and (PAAm/G/MA)-2 hydrogels. These hydrogels were chosen for the adsorption capacity study due to their characterization properties and MA contents. There are many studies in which MA is used to remove heavy metal ions [41]-[43]. According to literature, its carboxyl groups are responsible for the metal binding [41]. The electrostatic interaction occurs between the carboxylic groups of MA and heavy metal ions [44], [17]. This interaction form through the ion exchange mechanism. In addition, the oxygen in the carbonyl group of MA plays a role in the interaction of the metal ion with the polymer through the coordination bond [41], [43]. Therefore, the binding of metal ions to the polymer is proceed with the combined action of coordination, electrostatic interaction, and ion exchange [41]. Due to these properties, MA is frequently used in the removal of heavy metal ions.
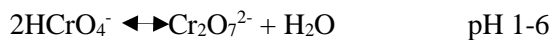
The effects of different initial feed Cr (VI) concentrations (C_i) on the adsorption capacity of (PAAm/G/MA)-1 and (PAAm/G/MA)-2 hydrogels were investigated in a range from 30 to150 mg/L at pH 1.0 for a period of 15h. The adsorption values (Q) of hydrogels are given in Figure 10. The adsorption increased directly with C_i, so it can be said that the adsorption depends on C_i. The results are compatible with the literature [44]. The number of adsorbed metal ions increases with an increase in C_i, so Q values are increased. No major differences were observed between the Q values of the (PAAm/G/MA)-1 and (PAAm/G/MA)-2 hydrogels. Q value of (PAAm/G/MA)-2 ranged from 28 to 117 mg/g, while Q value of (PAAm/G/MA)-1 ranged from 33 to 121 mg/g. This difference can be explained by the increment of crosslinking density in the structure slows down the penetration of water containing metal ion into the structure and so, the adsorption rate reduces [45].
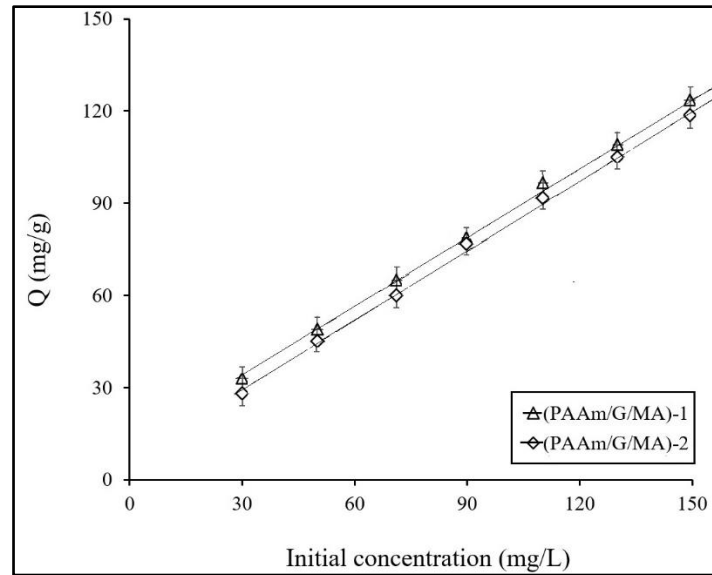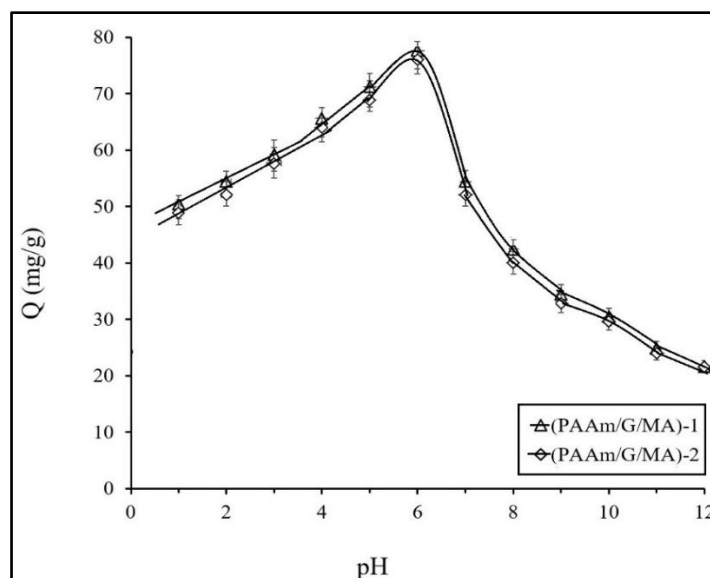
Figure 10. *The effect of initial concentration on the adsorption of Cr(VI)ions (under the conditions pH=1, temperature 25ºC in period of 900 min). Results shown are mean ± standard deviation, n = 3.*

pH is an important factor for adsorption methods. The effect of pH on the adsorption efficiency of (PAAm/G/MA)-1 and (PAAm/G/MA)-2 hydrogels, in the pH range 2–10, is given in Figure 11. Hydrogel was added to 50 mL of Cr (VI) solutions (80 mg/l) of different pH values. Initially, the adsorption increased speedily until pH 6. The maximum adsorption reached at pH 6. The adsorption steadily decreased thereafter. Similar findings for the adsorption of Cr (VI) with pH has been reported by Rengaraj et al. (2003) and Khan et al. (2017) with maximum adsorption reaching at pH 6 and 7, respectively [45], [46].

According to literature, Cr (VI) exists in various oxoanionic forms in aqueous solution at different pH values [43], [45]. Below pH 1.0, it is in the form of H_2CrO_4. Between pH 1–6, Cr (VI) is in the form of $HCrO_4^-$, which dimerizes to $Cr_2O_7^{2-}$ with the release of a water molecule into the environment [43], [46]. Cr (VI) is in the form of $Cr_2O_4^{2-}$ above pH 6. In other words, at higher pH values the ionized form is adsorbed, while at low pH the molecular form is adsorbed [47]. At pH 6, the reducing the $Cr_2O_7^{2-}$ and $HCrO_4^-$, and the forming of CrO_4^{2-} form is occurred; then, the electrostatic attraction is increased, and the adsorption capacity is enhanced too [47], [48]. Cr (VI) are adsorbed by the positively charged adsorbent surface up to pH 6. The decrease in the adsorption capacity after pH 6, dominant species are $HCrO_4^-$ and CrO_4^{2-}, can be explained by charge changes of the hydrogels from positive to negative, thus decreasing the electrostatic interaction between hydrogel to metal ions [46]-[48].

$2H_2CrO_4 \leftrightarrow 2H^+ + 2HCrO_4^-$ pH= 1

$2HCrO_4^- \leftrightarrow Cr_2O_7^{2-} + H_2O$ pH 1-6

$Cr_2O_7^{2-} + H_2O \leftrightarrow 2CrO_4^{2-} + 2H^+$ pH> 6

Figure 11. *The effect of pH on the adsorption of Cr(VI) ions (under the conditions initial Cr(VI) concentration of 80 mg/L, temperature 25°C in period of 900 min). Results shown are mean ± standard deviation, n = 3.*

The efficiency of contact time on the adsorption was researched and the equilibrium adsorption value was determined. It was clearly seen that time had a vital effect on adsorption. The results are displayed in Figure 12. The initial adsorption rate was high for both hydrogels. As the contact time increased, the metal ion uptake rate slowed down and then it reached a constant value. The results are compatible with the literature. According to literature, initially the functional groups of the hydrogels interact with metal ion easily. Thus, initial rate of adsorption is very high [49]. As the interaction continues, the adsorption rate slows down over time and eventually reaches a constant value. This time is defined as the equilibrium time [50]. During this time, a dynamic equilibrium occurs between the hydrogel and the solution; the adsorption rate is equal to the desorption rate from the hydrogel in the water, and the adsorption reaches equilibrium [49], [50]. The *Q* values of hydrogels increased gradually till 110 min and then the rate slowed down. The equilibrium adsorption value was found to be 75 mg/g for (PAAm/G/MA)-2 hydrogel, while the equilibrium adsorption value was found to be 78 mg/g for (PAAm/G/MA)-1 hydrogel.
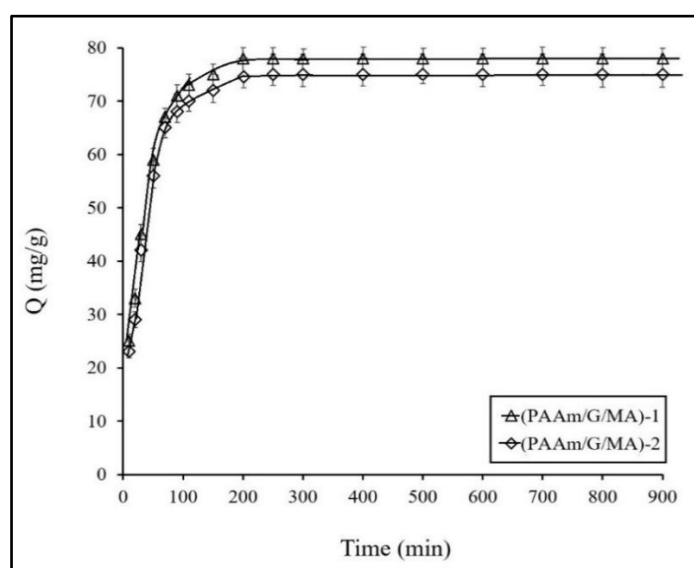

Figure 12. *The effect of contact time on the adsorption of Cr(VI) ions (under the conditions initial Cr(VI)concentration of 80mg/L, temperature 25°C and pH=1). Results shown are mean ± standard deviation, n = 3.*

Langmuir isotherm model was utilized with determining the adsorption isotherm [51], [52]. This Langmuir isotherm equation is given in Equation 5:

$$1/q_e = \frac{1}{Q^o x\, b\, x\, C_e} + \frac{1}{Q^o} \tag{5}$$

In Equation, the content of metal adsorbed is q_e (mg/g), the equilibrium concentration is C_e (mg/L), b and Q^o is Langmuir constants associated with energy of adsorption and adsorption capacity, respectively. The adsorption isotherm is given in Figure 13. If a plot of $1/q_e$ versus $1/C_e$ is plotted and a straight line is obtained and the calculated high correlation coefficient (R^2) of the graph is remarkably close to 1, the adsorption behavior can be assumed to fit the Langmuir isotherm. The intercept and the slope of this line then yield the constants b and Q^o, respectively. Q^o was found to be 555.55 and 322.58 mg/g for semi-IPN and full-IPN, respectively, while b was calculated as 0.0323 and 0.0563 L/mg for semi-IPN and full-IPN, respectively. The correlation coefficient (R^2) was found to be 0.9992 and 0.9984 for semi-IPN and full-IPN, respectively. The correlation coefficient displays a good accordance between parameters and indicates monolayer adsorption of metal ions on the adsorbent surface [51], [52].
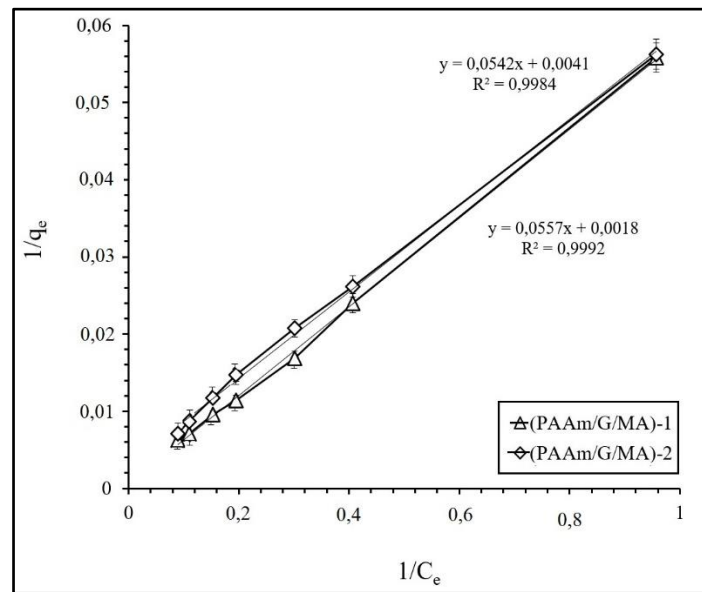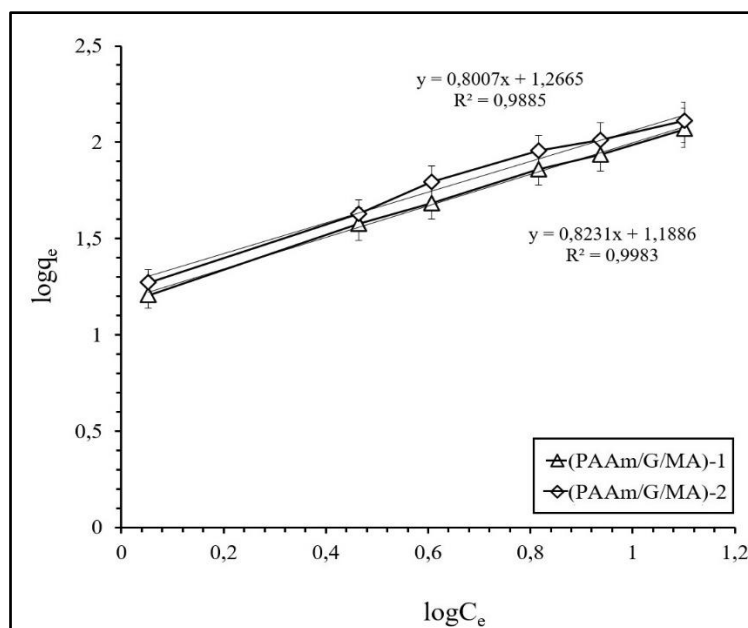

Figure 13. *Langmuir isotherm for adsorption of Cr (VI) ions (under the conditions pH=6, temperature 25ºC in period of 900 min).*

Freundlich isotherm displays in Equation 6 [9], [14]:

$$\log q_e = \log K_f + n log C_e \tag{6}$$

In Equation, the Freundlich constant is K_f, an adsorption capacity, depends on the binding energy. Freundlich coefficient is n, a heterogeneity factor, links to the deviation of adsorption from linearity. It can be detected from the plot of $log q_e$ vs. $log C_e$. The isotherm is displayed in Figure 14. n was found to be 0.8231 and 0.8007 mg/g for semi-IPN and full-IPN, respectively, while K_f was calculated as 15.44 and 18.47 for semi-IPN and full-IPN, respectively. The correlation coefficient (R^2) was found to be 0.9983 and 0.9885 for semi-IPN and full-IPN, respectively. R^2 values were over 0.96 indicating that the adsorption of Cr (VI) ions by semi and full-IPN hydrogel fitted also well on Freundlich isotherm. It can be said that the monolayer adsorption of the metal ions was occurred on the adsorbent surface [52]. Langmuir isotherm proved to be a better mathematical fit for equilibrium data than Freundlich model, based on the higher R^2 value.

Figure 14. *Freundlich isotherm for adsorption of Cr (VI) ions (under the conditions pH=6, temperature 25ºC in period of 900 min).*

IV. CONCLUSION

In this study, the gelatin (G)-polyacrylamide (PAAm)-based interpenetrating polymer network (IPN) hydrogels containing maleic acid (MA) was synthesized by free radical polymerization. The so-prepared hydrogel was utilized for removal of Cr (VI) from its aqueous solutions. The hydrogels were characterized by FTIR, TGA, DSC and SEM/EDX analysis. The degradation and mechanical behavior of hydrogels was also investigated. It was detected that IPN hydrogels had good water absorbency capability, degradation, mechanical, and thermal stabilities. Factors affecting the adsorption process such as pH, contact time, and initial concentration were extensively researched. It was observed that the extent of Cr (VI) adsorption increased with increasing initial Cr (VI) concentration within the range studied. It was found that adsorption of Cr (VI) by hydrogels was influenced by the increasing of the crosslinking amount in structure. Also, it was observed that the adsorption is pH-dependent and maximum sorption was obtained at pH 6. According to the study of the influence of contact time on the adsorption, a remarkable increase in Cr (VI) adsorption occurred up to 300 min. The adsorption data was determined to accord both Langmuir and Freundlich sorption isotherms, but Langmuir isotherm demonstrated to be a better mathematical fit for equilibrium data than Freundlich model, based on the higher the correlation coefficient value. The Langmuir adsorption capacity (Q) was determined to be 555.55 and 322.58 mg/g for semi-IPN and full-IPN, respectively. Freundlich constants, K_f, were found to be 15.44 and 18.47 for semi-IPN and full-IPN, respectively. According to results, it can be said that the synthesized IPN hydrogel could be utilized as metal adsorbents from aqueous solutions.

V. REFERENCES

[1]   P. Souda and L. Sreejith, "Poly (acrylate-acrylic acid-co-maleic acid) hydrogel: a cost effective and efficient method for removal of metal ions from water," *Separation Science and Technology,* c. 48, s. 18, ss. 2795-2803, 2013.

[2]   R. Torres-García, J. Flores-Estrada, J. V. Cauich-Rodríguez, M. Flores-Reyes and M. V. Flores-Merino, "Design of a polyacrylamide and gelatin hydrogel as a synthetic extracellular matrix." *International Journal of Polymeric Materials and Polymeric Biomaterials,* ss. 1-12, 2020.

[3]   A. Martínez-Ruvalcaba, F. Becerra-Bracamontes, J. C. Sánchez-Díaz and A.González-Alvarez, "Polyacrylamide-gelatin polymeric networks: effect of pH and gelatin concentration on the swelling kinetics and mechanical properties," *Polymer Bulletin,* c. 62, s. 4, ss. 539-548, 2009.

[4]   H. Ferfera-Harrar, N. Aiouaz and N. Dairi, "Synthesis and properties of chitosan-graft polyacrylamide/gelatin superabsorbent composites for wastewater purification.," *Polymer,* c. 6, s. 9, ss. 757-764, 2015.

[5]   M. Jaiswal, V. Koul, A. K. Dinda, S. Mohanty and K.G. Jain, "Cell adhesion and proliferation studies on semi-interpenetrating polymeric networks (semi-IPNs) of polyacrylamide and gelatin," *Journal of Biomedical Materials Research Part B: Applied Biomaterials,* c. 98, s. 2, ss. 342-350, 2011.

[6]   H. Kaşgöz, S. Özgümüş and M. Orbay, "Modified polyacrylamide hydrogels and their application in removal of heavy metal ions," *Polymer,* c. 44, s. 6, ss. 1785-1793, 2003.

[7]   O.V. Maikovych, N.G. Nosova, M.V. Yakoviv, À. Dron, A.V. Stasiuk, V.Ya. Samaryk, S.M. Varvarenko, S.A. Voronov, "Composite materials based on polyacrylamide and gelatin reinforced wıth polypropylene microfiber," *Voprosy khimii i khimicheskoi tekhnologii,* c. 1, ss. 45-54, 2021.

[8]   C. V. T. Rigueto, M. T. Nazari, L. A. Massuda, B. E. P. Ostwald, J. S. Piccin and A. Dettmer, "Production and environmental applications of gelatin-based composite adsorbents for contaminants removal: a review," *Environmental Chemistry Letters*, ss. 1-22, 2021.

[9]   H. S. Jamwal, S. Ranote, D. Kumar, G. S. Chauhan, and M. Bansal, "Gelatin-based mesoporous hybrid materials for Hg^{2+} ions removal from aqueous solutions," *Separation and Purification Technology,* c. 239, ss. 116513, 2020.

[10]   K. Sangeetha, G. Vidhya G. Vasugi, E.K. Girija, "Lead and cadmium removal from single and binary metal ion solution by novel hydroxyapatite/alginate/gelatin nanocomposites," *Journal of Environmental Chemical Engineering,* c. 6, ss. 1118–1126, 2018.

[11]   M. E. Mahmoud, R. H. A. Mohamed, "Biosorption and removal of Cr (VI)–Cr (III) from water by eco-friendly gelatin biosorbent," *Journal of Environmental Chemical Engineering,* c. 2, s. 1, ss. 715-722, 2014.

[12]   S. Perumal, R. Atchudan, D.H. Yoon, J. Joo, I. W. Cheong, "Graphene oxide-embedded chitosan/gelatin hydrogel particles for the adsorptions of multiple heavy metal ions," *Journal of Materials Science,* c. 55, s. 22, ss. 9354-9363, 2020.

[13]   A. K. Bajpai and H. Bundela, "Influence of gelatin on the properties of hydroxyapatite–polyacrylamide nanocomposite as a potential bone substitute," *Composite Interfaces,* c. 15, s. 7-9, ss. 709-729, 2008.

[14]   M. P. Das, P. R. Suguna, K. Prasad, J. V. Vijaylakshmi and M. Renuka, "Extraction and characterization of gelatin: a functional biopolymer," *International Journal of Pharmacy and Pharmaceutical Sciences,* c. 9, s. 239, ss.10-22159, 2017.

[15]   Y. C. Lin, C. C. Wang and C. W. Tung, "An in silico toxicogenomics approach for inferring potential diseases associated with maleic acid," *Chemico-Biological Interactions*, c. 223, ss. 38-44, 2014.

[16]   A. G. Ibrahim, A. S. Saleh, E. M. Elsharma, E., Metwally and T. Siyam, "Chitosan-g-maleic acid for effective removal of copper and nickel ions from their solutions," *International Journal Of Biological Macromolecules,* c. 121, ss. 1287-1294, 2019.

[17]   W. Maatar and S. Boufi, "Poly (methacylic acid-co-maleic acid) grafted nanofibrillated cellulose as a reusable novel heavy metal ions adsorbent," *Carbohydrate Polymers,* c. 126, ss. 199-207, 2015.

[18]   A. M. Patel, R. G. Patel and M. P. Patel, "Super Absorbent Hydrogel Based on Poly [acrylamide/maleic   acid/2-methacryloxy   ethyl   trimethylammonium   chloride]:   Synthesis, Characterization and their Application in the Removal of Chromium (VI) from Aqueous Solution," *Journal of Macromolecular Science, Part A,* c. 48, s. 5, ss. 339-347, 2011.

[19]   E. Helvacıoğlu, V. Aydın, T. Nugay, N. Nugay, B. G. Uluocak and Şen, S, "High strength poly (acrylamide)-clay hydrogels," *Journal of Polymer Research*, c. 18, s. 6, ss. 2341-2350, 2011.

[20]   M. A. Paul, C. Delcourt, M. Alexandre, P. Degée, F. Monteverde and P. Dubois, "Polylactide/montmorillonite nanocomposites: study of the hydrolytic degradation," *Polymer Degradation and Stability,* c. 87, s. 3, ss. 535-542, 2005.

[21]   E. A. Kamoun, E. R. S. Kenawy, T. M. Tamer, M. A. El-Meligy and M. S. M. Eldin, "Poly (vinyl alcohol)-alginate physically crosslinked hydrogel membranes for wound dressing applications: characterization and bio-evaluation," *Arabian Journal of Chemistry,* c. 8, s. 1, ss. 38-47, 2015.

[22]   M. A. Paul, C. Delcourt, M. Alexandre, P. Degée, F. Monteverde and P. Dubois, "Polylactide/montmorillonite nanocomposites: study of the hydrolytic degradation," *Polymer Degradation and Stability,* c. 87, s. 3, 535-542, 2005.

[23]   T. Caykara, C. Özyürek, Ö. Kantoğlu and B. Erdoğan, "Thermal behavior of poly (2-hydroxyethyl methacrylate-maleic acid) networks," *Polymer Degradation and Stability,* c.80, s. 2, ss. 339-343, 2003.

[24]   B. Grabowska, M. Holtzer, S. Eichholz, K. Hodor, and A. Bobrowski, "Thermal analysis of a sodium salt of the maleic acid-acrylic acid copolymer used as a polymeric binder," *Polimery,* c. 56, s. 2, ss. 151-155, 2011.

[25]   A. Enumo Jr, I. P. Gross, R. H. Saatkamp, A. T. Pires and A. L. Parize, "Evaluation of mechanical, thermal and morphological properties of PLA films plasticized with maleic acid and its propyl ester derivatives," *Polymer Testing,* c. 88, s.106552, ss. 1-9, 2020.

[26]   G. O. Akalin, O.O. Taner and T. Taner, "The preparation, characterization and antibacterial properties of chitosan/pectin silver nanoparticle films," *Polymer Bulletin,* ss. 1-18, 2021.

[27]   J. Maity, and S. K. Ray, "Enhanced adsorption of Cr (VI) from water by guar gum based composite hydrogels, " *International journal of biological macromolecules*, c. 89, ss. 246-255, 2016.

[28]   T.A. Khan, M. Nazir, I. Ali and A. Kumar, "Removal of chromium (VI) from aqueous solution using guar gum–nano zinc oxide biocomposite adsorbent," Arabian Journal of Chemistry, c. 10, ss. 2388-2398, 2017.

[29]   M. Eid, M. A. Abdel-Ghaffar and A. M. Dessouki, "Effect of maleic acid content on the thermal stability, swelling behaviour and network structure of gelatin-based hydrogels prepared by gamma irradiation," *Nuclear Instruments and Methods in Physics Research Section B,* c. 267, s. 1, ss. 91-98, 2009.

[30]   A. B. D. Nandiyanto, R. Oktiani and R. Ragadhita, "How to read and interpret FTIR spectroscope of organic material," *Indonesian Journal of Science and Technology*, c. 4, s. 1, ss. 97-118, 2019.

[31]   A. Jafari, S. Hassanajili, F. Ghaffari and N. Azarpira, "Modulating the physico-mechanical properties of polyacrylamide/gelatin hydrogels for tissue engineering application," *Polymer Bulletin,* ss. 1-22, 2021.

[32]   S. Belkadi, H. Bendaikha, F. Lebsir and S. Ould-Kada, "Synthesis, characterization and swelling study of poly (methacrylic acid-co-maleic acid) hydrogels," *Oriental Journal of Chemistry,* c. 34, s. 2, ss. 948-954, 2018.

[33]   M. M. Ghobashy, B. K. El-Damhougy, N.Nady, H. Abd El-Wahab, A. M. Naser and F. Abdelhai, "Radiation crosslinking of modifying super absorbent (polyacrylamide/gelatin) hydrogel as fertilizers carrier and soil conditioner," *Journal of Polymers and the Environment,* c. 26, s. 9, ss. 3981-3994, 2018.

[34]   S. Bennour and Louzri, F, "Study of swelling properties and thermal behavior of poly (N, N-dimethylacrylamide-co-maleic acid) based hydrogels," *Advances in Chemistry,* ss. 1-10, 2014.

[35]   Y. F. Buys, A. N. A. Aznan, and H. Anuar, Mechanical properties, morphology, and hydrolytic degradation behavior of polylactic acid/natural rubber blends," *In IOP Conference Series: Materials Science and Engineering,* c. 290, s., ss.1-8. 2018.

[36]   E. A. Kamoun, E. R. S. Kenawy, T. M. Tamer, M. A. El-Meligy and M. S. M. Eldin, "Poly (vinyl alcohol)-alginate physically crosslinked hydrogel membranes for wound dressing applications: characterization and bio-evaluation," *Arabian Journal of Chemistry,* c. 8, s. 1, ss. 38-47, 2015.

[37]   C. Xiao, Y. Lu, Z. Jing, L. Zhang, "Study on physical properties of blend films from gelatin and polyacrylamide solutions," *Journal of Applied Polymer Science,* c. 83, s. 5, ss. 949–955, 2002.

[38]   J. Filipović, L. Katsikas, I. Popović, S. Veličković, T. Djakov and D. Petrović-Djakov, "The thermal degradation of some alkali metal salts of poly (itaconic acid)," *Journal of Thermal Analysis and Calorimetry,* c. 49, s. 1, ss. 335-341, 1997.

[39]   M.C. Chandy, V.N. Pillai, "Water sorption and water binding properties of crosslinked polyacrylamides: effect of macromolecular structure and crosslinking," *Polymer International,* c. 37, s. 1, ss. 39–45, 1995.

[40]   A.N. Fraga, R.J., Williams, "Thermal properties of gelatin films," *Polymer*, c. 26, s. 1, ss. 113–118, 1985.

[41]   A. G. Ibrahim, A. S. Saleh, E. M. Elsharma, E. Metwally, and T. Siyam, "Chitosan-g-maleic acid for effective removal of copper and nickel ions from their solutions," *International Journal of Biological Macromolecules,* c. 121, ss. 1287-1294, 2019.

[42]   Y. R. Qiu and L. J. Mao, "Removal of heavy metal ions from aqueous solution by ultrafiltration assisted with copolymer of maleic acid and acrylic acid," *Desalination,* c. 329, ss. 78-85, 2013.

 [43]   A. R. Allafchian, A. Shiasi and R. Amiri, "Preparing of poly (acrylonitrile co maleic acid) nanofiber mats for removal of Ni (II) and Cr (VI) ions from water," *Journal of the Taiwan Institute of Chemical Engineers,* c. 80, ss. 563-569, 2017.

[44]   J. Maity, and S. K. Ray, "Enhanced adsorption of Cr (VI) from water by guar gum based composite hydrogels," *International Journal of Biological Macromolecules,* c. 89, ss. 246-255, 2016.

[45]   S. Rengaraj, C. K. Joo, Y. Kim and J. Yi, "Kinetics of removal of chromium from water and electronic process wastewater by ion exchange resins: 1200H, 1500H and IRN97H," *Journal of Hazardous Materials*, c. 102, s. 2-3, ss. 257-275, 2003.

[46]   T. A. Khan, M. Nazir, I. Ali and A.Kumar, "Removal of chromium (VI) from aqueous solution using guar gum–nano zinc oxide biocomposite adsorbent," *Arabian Journal of Chemistry,* c. 10, ss. 2388-2398, 2017.

[47]   K. G. Bhattacharyya and S. Sen Gupta, "Adsorption of chromium (VI) from water by clays," *Industrial & Engineering Chemistry Research,* c. 45, s. 21, ss. 7232-7240, 2006.

[48]   Y. Lei, H. Su, F. Tian, "A novel nitrogen enriched hydrochar adsorbents derived from salix biomass for Cr (VI) adsorption," *Scientific reports,* c. 8, s. 1, ss. 1-9, 2018.

[49]   J. Maity, S. K. Ray, "Enhanced adsorption of Cr (VI) from water by guar gum based composite hydrogels," *International journal of biological macromolecules,* c. 89, ss. 246-255, 2016.

[50]   S. K. Bajpai, S. Johnson, "Poly (acrylamide-co-maleic acid) hydrogels for removal of Cr (VI) from aqueous solutions, Part 1: Synthesis and swelling characterization," *Journal of Applied Polymer Science,* c. 100, s. 4, ss. 2759-2769, 2006.

[51]   Ö. B. Üzüm, S. Kundakci, and E. Karadağ, "Uranyl ion uptake from aqueous solutions by chemically cross-linked polyelectrolyte CAMA hydrogels," *Polymer-Plastics Technology and Engineering,* c. 46, s. 8, ss. 775-780, 2007.

[52]   I. Langmuir, "The adsorption of gases on plane surfaces of glass, mica and platinum," *Journal of the American Chemical Society,* c. 40, s. 9, ss. 1361-1403, 1918.